scientific reports

Check for updates

OPEN

Assessment of solar energy potential for Bahir Dar city, Ethiopia

Aschale Getnet[1], Tereche Getnet[1], Assefa Beyene[1], Ramesh Babu Nallamothu[2]✉, Tewodros Semeneh[1] & Hailemariam Mulugeta[1]

The world's energy consumption is being replaced by renewable energies in large part because of the depletion of fossil fuels and the acceleration of environmental change. This study reports the amount of inward solar radiation in the date range from January 2018 to December 2022 in the Gregorian Calendar for certain areas in Bahir Dar, Ethiopia: 37°E and 11.6°N. On the horizontal surface of the case area, the month with the highest global radiation (monthly average daily) is March, at approximately 42.56 MJ/m^2. day; June has the lowest diffuse radiation, at 16.2 MJ/m^2.day. Furthermore, April had the most global radiation (monthly average hourly) on the horizontal surface, measuring 9.09 MJ/m2.hour, while June had the lowest diffuse radiation, measuring 2.3 MJ/m2.hour. In addition, this study predicts the beam, diffuse, and total radiation on the tilted collector using the total available horizontal radiation on a monthly and hourly basis. According to the research, the output of the radiation on the tilted surface towards the equator in the northern hemisphere, azimuth angle, γ = 0°, shows that the highest possible total radiation (monthly average daily) is 48.3 MJ/m^2. day (January) and the highest possible total radiation (monthly average hourly) in February, 9.14 MJ/m^2.hour at 1:00 p.m.

Keywords Beam solar radiation, Diffuse solar radiation, Global solar radiation, Sunshine hour

Recently, due to the advantage of renewable energy technologies, increasing the cost of fossil fuels, and its global warming effect, the use of distributed energy sources has been growing[1]. Moreover, accessibility to electric power results in social, economic, and technological advances. In the recent decade, the thermal energy demand has increased considerably because of urbanization, changes in lifestyles and consumption patterns[2]. On the other hand, due to environmental concerns, the use of renewable energies has received more attention.

To utilize solar energy, sunlight is converted into usable energy forms (heat or electricity). Generally, there are two different technologies namely photovoltaic panels (PV) and concentrated solar power (CSP) for electricity generation[3]. The CSP technology uses concentrated solar radiation as a high-temperature thermal energy source to drive steam turbines and convert them to electricity[4,5]. These systems are appropriate for the areas where direct solar radiation is available and also the number of clear sunny days in the year is high[6,7]. As well, PV technology is a power system based on PV cells that converts solar energy into electricity. Annually, considering the PV market growing by 30–40%, the PV system is turned into one of the most important energy carriers by appropriate technologies[5,30].

Solar energy utilization can offset the increasing greenhouse gas emission from non-renewable sources and subsequent increase in global mean temperature as a result of climate change[8]. One of the biggest challenges facing the solar energy industry is scarcity of data at specific locations. In developing countries like Ethiopia, solar radiation data are unavailable mainly due to a lack of instrumentation[9]. In such situations, theoretical models are used to estimate solar radiation, with inputs from observations[10]. Observations such as sunshine duration usually serve as input for measuring solar radiation, though they have limited spatial coverage. Solar radiation climatologists have identified cloud cover as a metric for solar radiation estimation because cloud cover information is more geographically covered than sunshine duration[11]. The solar radiation reaching the earth's surface is attenuated by the presence of clouds, dust, smoke, atmospheric chemical compounds, and water vapor. Dust, in particular, is a major challenge to the efficient harnessing of solar energy during the dry seasons in tropical regions such as sub-Saharan Africa[12,13]. The solar beam attenuated by these suspended atmospheric substances, especially clouds depends on the cloud type and layers, cloud thickness, and altitude. An important parameter to consider in assessing the performance of solar PV installations is the extra-terrestrial radiation

[1]Faculty of Mechanical and Industrial Engineering, Bahir Dar Institute of Technology, Bahir Dar University, Bahir DarP.O. Box 26, Ethiopia. [2]Department of Mechanical Engineering, College of Mechanical Chemical and Materials Engineering, Adama Science and Technology University, Adama, Ethiopia. ✉email: ramesh.babu@astu.edu.et

reaching the top of the Earth's atmosphere from the sun[14]. This radiation is fast depleting in the atmosphere due to absorption, reflection, and scattering[15]. The amount of radiation that eventually gets to the Earth's surface is known as global solar radiation.

Among the renewable sources, solar energy is presented as the ideal alternative to face energy change, with a multitude of technologies being developed to meet this demand. Solar resources can generate enough energy to supply the planet, and electricity can be obtained directly from photovoltaic modules[16,29]. Solar energy has registered 2020 a percentage close to 39% in terms of global participation, implying that more than one-third of the power plants are solar.

The energy generated by PV modules depends on several variables, such as the intensity of solar irradiance, ambient temperature, wind speed, module positioning and ventilation, environmental dust and pollution, and shadowing[17]. Although most of Africa receives over 2000 kWh/m2 of global solar radiation annually, Ethiopia has not fully capitalized on solar energy-generating plants on the continent. Due to its proximity to the equator, Ethiopia enjoys abundant solar resources. Accurate estimations of solar radiation are crucial for successful PV power generation in the region[18].

The initial goal of compiling the dataset on solar energy potential assessment for Bahir Dar City, Ethiopia was to investigate the amount of incoming solar radiation in a specific location and timeframe. The dataset aimed to provide useful information for solar energy research and applications. The data collection process included recording survey results and measuring various solar radiation parameters. The dataset is significant in the context of renewable energy and the growing interest in environmentally friendly alternatives to fossil fuels. This data provides valuable insights that can help drive the transition towards more sustainable energy sources.

The dataset contributes to understanding the availability and characteristics of solar radiation in the region by assessing the solar energy potential in Bahir Dar City. The dataset can be used in a variety of applications, including climate modeling, agricultural planning, and the optimization of solar panel locations for solar energy producers. Researchers studying the potential of solar radiation on horizontal surfaces can also use this dataset to estimate solar radiation for different collector tilt angles. Furthermore, the dataset is useful for calculating the efficiency of incoming solar radiation. Overall, the dataset was compiled to aid solar energy research, forecast future solar energy prospects, and aid in the development of sustainable energy solutions in Bahir Dar, Ethiopia.

1.1. Study objectives

The primary objectives of this study were to:

- Assess the solar energy potential in Bahir Dar City by analyzing the availability and characteristics of solar radiation in the region.
- Provide useful information to support solar energy research and applications in the area.
- Contribute to the understanding of solar radiation patterns on horizontal and tilted surfaces, which can aid in the optimization of solar panel installations and the calculation of system efficiencies.

1.2. Data value

The dataset compiled for this study can be used in a variety of applications, including climate modeling, agricultural planning, and the optimization of solar panel locations for solar energy producers. Researchers studying the potential of solar radiation can also utilize this dataset to estimate solar radiation for different collector tilt angles. Overall, this dataset was compiled to aid solar energy research, forecast future solar energy prospects, and support the development of sustainable energy solutions in Bahir Dar, Ethiopia.

The radiation values offered by this dataset provide useful data for several applications, including climate modeling, agricultural planning, and the generation of solar energy. Companies that provide solar energy, for instance, can use this information to optimize the location and effectiveness of solar panels. The data will also help researchers determine the city of Bahir Dar's greatest horizontal solar radiation potential and choose the best locations for solar panel installations based on the availability of solar radiation. Additionally, researchers studying the solar radiation potential on horizontal surfaces can use this dataset to estimate solar radiation for different collector tilt angles.

Researchers can further investigate this dataset, conduct additional analysis, and build on the findings to advance their own research goals. They can also compare this dataset to others to evaluate the performance, effectiveness, or impact of various models, methodologies, or interventions. Furthermore, policymakers, industry professionals, and practitioners can use the insights from this dataset to inform evidence-based decision-making, develop strategies, and shape interventions related to renewable energy and sustainable development in the region.

2. Experimental design, materials and methods

2.1. Location of the study area

Bahir Dar is situated in the northwestern region of Ethiopia, nestled along the southern shore of Lake Tana, the largest lake in the country. The city lies at an average elevation of around 1,800 m (5,906 feet) above sea level, within the Ethiopian Highlands. The latitude of 11°36'N situates Bahir Dar well within the tropical climate zone, while the longitude of 37°23'E positions the city in the eastern region of Africa, adjacent to the Great Rift Valley.

Furthermore, the solar radiation characteristics of Bahir Dar, Ethiopia situated at a latitude of 11°36'N, Bahir Dar experiences high solar angles throughout the year, with the sun reaching its zenith near the equinoxes. This high solar angle, combined with the tropical latitude, results in relatively high levels of incoming solar radiation. The high elevation of Bahir Dar, approximately 1,800 m (5,906 feet) above sea level, also plays a role in the solar radiation dynamics. The thinner atmosphere at higher elevations typically allows for greater transmission of solar radiation, leading to increased surface insolation compared to lower-lying areas.

2.2. Meteorological parameters and instrumentation

The researcher employed a Campbell-Stokes sunshine recorder, Prior to deployment, the sunshine recorder underwent a thorough calibration process in line with the manufacturer's guidelines, including checking the alignment, inspecting the glass sphere, and verifying the accuracy against a reference standard. To maintain the sunshine recorder's performance, the researchers instituted a regular maintenance and cleaning regimen. They also implemented a cross-checking procedure, comparing the sunshine duration data with concurrent solar radiation measurements obtained from a pyranometer. For the pyranometers, the researchers applied rigorous calibration and quality assurance measures, adhering to the manufacturers' recommended procedures and using traceable standards. They conducted periodic calibration checks and implemented comprehensive data quality control processes, including visual inspection, range checks, and statistical analyses, to detect and filter out erroneous or suspicious data points, and performed regular maintenance to ensure the continued accuracy and reliability of the measurements. Additional information about Atmospheric & Astronomical Parameters and suitability of estimation of monthly average diffuse solar radiation can be found in[31,32].

2.2.1. Specification

Pyranometer Specifications: Model: Kipp & Zonen CMP11 Pyranometer, Spectral range of 285 to 2800 nm, Sensitivity of 7 to 14 μV/W/m², Response time of less than 5 s, Zero offset A of less than 7 W/m², Zero offset B of less than 2 W/m², Directional error (up to 80° with 1000 W/m² beam) of less than 10 W/m², Temperature dependence of sensitivity (between −10 °C to +40 °C) of less than 1%, Operating temperature range of -40 °C to +80 °C, Maximum solar irradiance of 4000 W/m², and a Field of view of 180 degrees.

Data Logger Specifications: Model: Campbell Scientific CR1000X Measurement and Control Datalogger, Analog inputs: 16 single-ended or 8 differentials, Scan rate: Up to 100 Hz, Memory: 4 MB of battery-backed SRAM, 4 GB of flash, Operating temperature range: -40 °C to +70 °C, Measurement types: Voltage, current, resistance, thermocouple, RTD, thermistor, frequency, Data storage: Memory card or built-in flash, Communication options: Ethernet, RS-232, RS-485, USB.

2.2.2. Configuration

The pyranometer would be connected to one of the analog input channels on the CR1000X data logger as shown on Fig. 1. The data logger programmed to read the pyrometer output voltage in every minute and store the solar radiation data (in W/m²) on the data storage device.

2.3. Solar data assessment

Solar data assessment in Bahir Dar City, and provides compelling evidence to support its credibility in the field of solar energy. The dataset has the potential to provide novel insights and further research in this field. The data was collected using specialized instruments designed to capture the specific phenomenon or parameters of interest. We were able to obtain data with unprecedented precision and accuracy by using a sunshine recorder device. Furthermore, our dataset covers a spatial or temporal scope that has not previously been extensively researched. We discovered valuable data that sheds light on previously unknown dynamics by focusing on a specific geographic region or period. This uniqueness broadens the field's knowledge base and opens up new avenues for insights and discoveries.

In addition, implemented rigorous validation and quality assurance procedures throughout the data collection process to ensure the reliability and accuracy of our dataset. When compared to other datasets in the field, our dataset stands out due to its distinct features. It provides for a specific geographical location called Bahir Dar city and covers five years from 2018 to 2022 and the dataset makes an important contribution to the field by filling research gaps and supplementing existing knowledge.

This dataset has numerous potential applications and implications. Its uniqueness opens new research avenues, informs evidence-based decision-making, and supports practical applications for agriculture and solar panel installation in and around the studied zone that the dataset will be useful to researchers, policymakers, and practitioners alike. This dataset, solar data assessment in Bahir Dar city, exemplifies our commitment to advancing knowledge and understanding of solar energy. Its uniqueness, backed up by our meticulous data collection and distinguishing features, makes it a valuable asset for further research and exploration.

The assessment of solar energy potential in Bahir Dar, Ethiopia, used a systematic and comprehensive experimental design to estimate incoming solar radiation and provide valuable insights for solar energy research and applications. Bahir Dar City, located at 37° E and 11.6° N, was carefully chosen as the study location. During the site selection process, factors such as geographical coordinates, altitude (approximately 1800 m above sea

Fig. 1. Processing of radiation data at Bahir Dar, Ethiopia.

level), and other relevant characteristics were considered. The data collection period lasted from 2018 to 2022 G.C. This long-term data collection strategy allowed for a thorough examination of solar radiation patterns and trends, taking seasonal and annual variations into account.

To ensure accurate measurements and reliable results a local weather station near the study area was critical in providing meteorological data. The weather station recorded parameters such as humidity, wind speed, and rainfall. This extra meteorological data was critical in determining the relationship between solar radiation and current weather conditions.

The sensors were calibrated regularly to ensure the accuracy and reliability of the measurements. During the calibration process, the sensors' readings were compared to a known reference source of solar radiation, ensuring precise and consistent measurements throughout the data collection period.

Estimation of available solar radiation on horizontal and tilt surfaces from five years of average sunshine hour duration is shown in Table 1 for Bahir Dar city over five years (2018–2022), which derived from the primary data recorded by our research team presented on Table 2.

Solar radiation value reached on the surface of the earth varies based on both geography and climate conditions of the case area. The total solar radiation available on the surface is the aggregate of the beam, diffuse radiation, and the reflected radiation from the inclined surface. The hourly radiation is derived from the daily radiation on the horizontal/ tilt surface[1].

The radiation on extraterrestrial surfaces is estimated by the Modified Angstrom-type regression equation using Eq. (1)[8]. Horizontal surface daily radiation is estimated using Eq. (3).

$$H_o = \frac{24 * 3600 * G_{sc}}{\pi}(1 + 0.003\cos\frac{360n}{365}(\cos\varphi \cos\delta \sin\omega_s + \frac{\pi\,\omega_s}{180}\sin\delta \sin\varphi)). \quad (1)$$

The sunrise hour angle is calculated as;

$$\omega_s = cos^{-1}(-tan\phi\, tan\delta) \quad (2)$$

$$\frac{H}{H_o} = a + b\left(\frac{\bar{n}_s}{\bar{N}_s}\right) \quad (3)$$

Where,

$$\delta = 23.45\sin\left(360\frac{284 + n}{365}\right) \quad (4)$$

$\bar{H}_o$, Horizontal surface Monthly Average extraterrestrial radiation in MJ/m^2.day.
$G_{sc} = 1367\ \frac{W}{m^2}$ (Solar Constant)
$\bar{H}$,, Horizontal surface Monthly Average daily radiation in MJ/m^2.day.
$\bar{n}_s$- Monthly average daily sunshine hours.

2.4. Data description

The analysis of solar radiation in different forms (Global, Diffuse, and Beam radiation on a daily and hourly basis) on either horizontal surface/tilt surface helps to predict the efficiency of the thermal process[1].

Sunshine hours measure thelength of time on Earth that is sunny in a particular time (generally, a day or a year) and is typically represented as an average value over several years. It measures the total energy that sunshine delivers over a certain time, in that it provides an indicator of how cloudy a place is[5]. Five years of sunny hours are shown in Table 2 together with the five-year average sunshine hours from recorded data in Table 1;

Months	Average (2018–2022)
January	9.8
February	9.6
March	9.34
April	9.12
May	8.23
June	7.86
July	5.24
August	4.4
September	6.54
October	8.42
November	9.72
December	9.94

Table 1. Sunshine hour duration.

Months	January	February	March	April	May	June	July	August	September	October	November	December
2018	9.7	10.1	9.3	9.8	8.6	6.6	4.2	2.9	6.8	8.3	9.7	9.9
2019	9.8	9.8	9.1	7.9	7.7	6.9	4.9	4.7	6	8.6	9.7	9.7
2020	9.6	9.7	9.8	9.9	8.4	6.8	7.1	5.6	6.7	8.8	9.4	9.8
2021	9.7	10	9.5	9.1	7.1	7.4	4.5	4.6	6.4	8.7	9.8	10
2022	10.2	8.4	9	8.9	7.5	7.3	5.5	4.2	6.8	7.7	10	10.3

Table 2. Hourly sunshine duration.

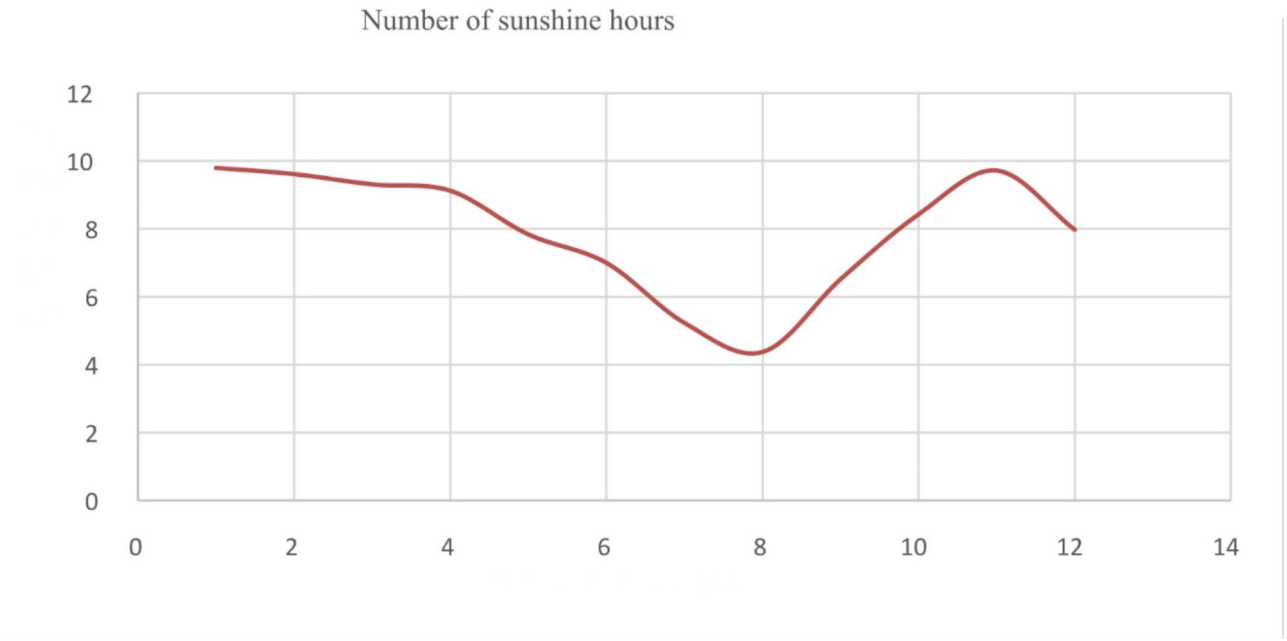

Fig. 2. Number of sunshine hours Vs months.

Month	Average (2018–2022)
January	39.1
February	41.5
March	42.6
April	42.3
May	36.8
June	33.3
July	27.3
August	24.6
September	31.9
October	36.6
November	38.3
December	32.1

Table 3. Horizontal surface global radiation (MJ/m2 /day). (Monthly Average daily).

Fig. 2[9]. Tables 3 and 4, and Table 5 present the solar radiation reached on the horizontal surface, i.e. Monthly average daily beam, diffuse, and global radiation respectively, and Fig. 3 compares these data. In addition, the declination angle of each month for the case area depicted on Fig. 4 as well as equation of time for each month with time is presented on Fig. 5.

Figure 6 indicates sunshine hours length $\bar{N}_s$computed from Cooper's formula.

$$\bar{N}_s = \left(\frac{2}{15}\right)\omega_s \tag{5}$$

$$a = -0.0110 + 0.235\cos\varphi + 0.323\left(\frac{\bar{n}_s}{\bar{N}_s}\right) \tag{6}$$

$$b = 1.449 - 0.533\cos\varphi - 0.0.694\left(\frac{\bar{n}_s}{\bar{N}_s}\right) \tag{7}$$

Moreover, monthly average daily radiation

$$\frac{H_d}{H} = 0.931 - 0.814 \times \left(\frac{\bar{n}_s}{\bar{N}_s}\right) \tag{8}$$

Month	Average (2018–2022)
January	30.0
February	30.7
March	29.8
April	28.4
May	21.2
June	17.2
July	11.1
August	8.8
September	16.3
October	24.1
November	29.2
December	20.6

Table 4. Horizontal surface diffuse radiation (MJ/m^2/day). Monthly average daily.

Month	Average (2018–2022)
January	9.12
February	10.8
March	12.7
April	13.8
May	15.6
June	16.0
July	16.2
August	15.8
September	15.6
October	12.5
November	9.1
December	11.5

Table 5. Horizontal surface beam radiation (MJ/m^2/day). Monthly average daily.

2.5. Hourly solar radiation from daily data

Using the equation of Collares Pereira and Rabl, horizontal surface hourly global radiation is estimated from the daily global radiation[20].

$$\frac{I}{H} = \frac{\pi}{24}(a + b\cos\omega\ )\left(\frac{\cos\omega\ - \cos\omega_{\ s}}{\sin\omega_{\ s} - \frac{\pi\ \omega_{\ s}}{180}\cos\omega_{\ s}}\right) \tag{9}$$

Where a and b,

$$a = 0.409 + 0.5016\ sin\ \omega_s - 60 \tag{10}$$

$$b = 0.6609 - 0.4767\ sin\ \omega_s - 60 \tag{11}$$

Hour angle (ω) and sunset hour angle (ωs) are in degrees.

Likewise, Liu and Jordan calculate the hourly diffuse radiation from the average daily diffuse.

Radiation

$$\frac{I_d}{\bar{H}_d} = \frac{\pi}{24}\left(\frac{\cos\omega\ - \cos\omega_{\ s}}{\sin\omega_{\ s} - \frac{\pi}{180}\omega_{\ s}\cos\omega_{\ s}}\right) \tag{12}$$

3. Results and discussion

3.1. Solar radiation on horizontal surface data description

The dataset aimed to articulate the available beam, diffuse and global radiation in the city Bahir Dar, Ethiopia. As per this investigation, the following figure description shows detail available radiation values.

Figure 4 describes Monthly Average Beam, Diffuse and Global solar radiation for each representative day of a year months. Thus,

- Maximum available beam radiation – 30.4 MJ/m^2.day (February).

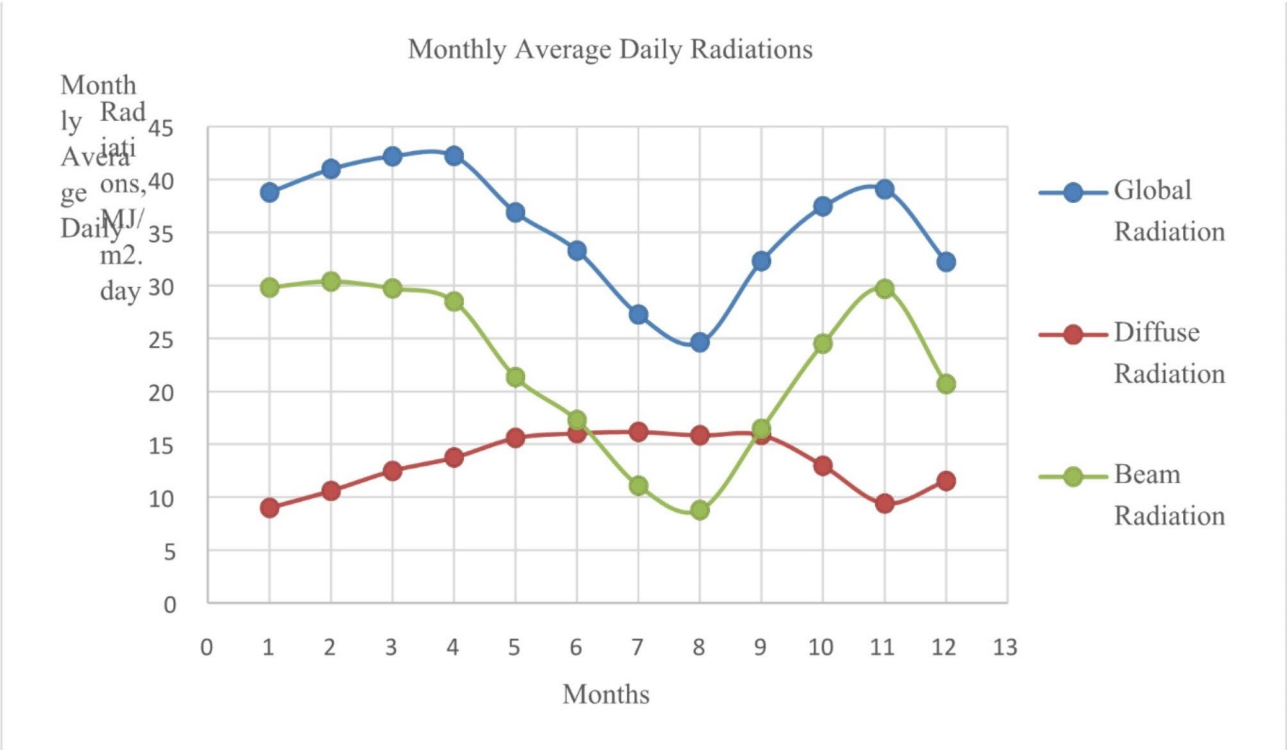

Fig. 3. Monthly Variation of Horizontal Surface Beam, Diffuse and Global Solar Radiation.

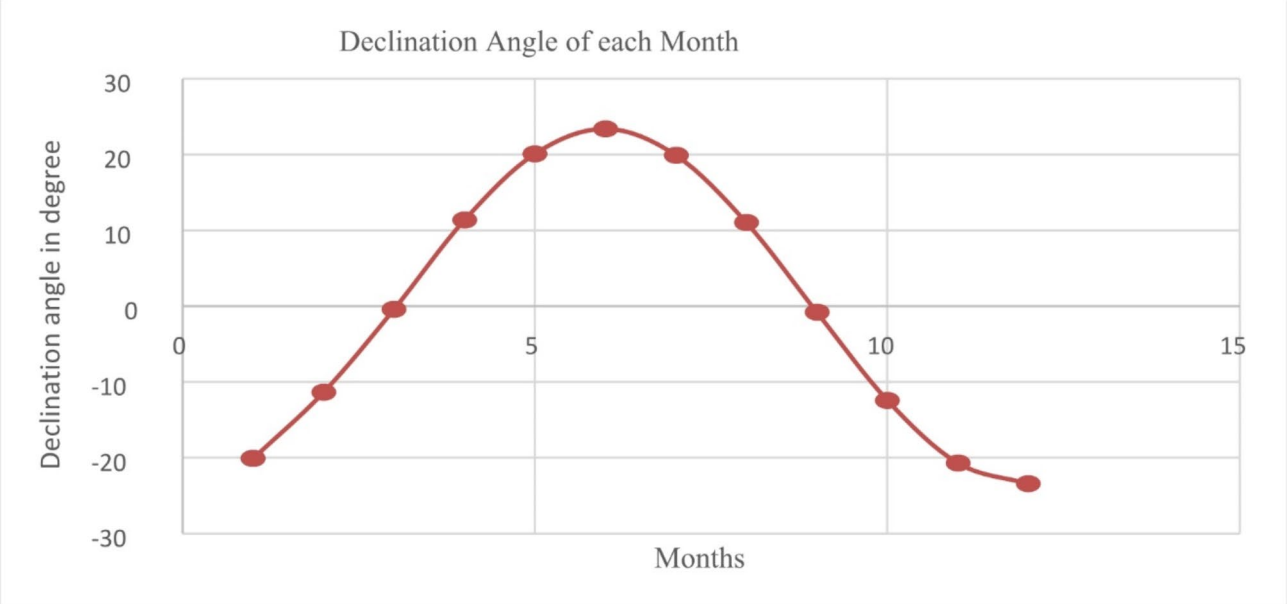

Fig. 4. Declination angle.

- Minimum available beam radiation – 8.8 MJ/m^2.day (August).
- Maximum available diffuse radiation – 16.15 MJ/m^2.day (July).
- Minimum available diffuse radiation – 8.98 MJ/m^2.day (January).
- Maximum available global radiation – 42.56 MJ/m^2.day (April).
- Minimum available global radiation – 24.6 MJ/m^2.day (August).

Figure 5 shows number of sunshine hours Vs months. Figure 7 shows that the average hourly global radiation for each representative day of months in a year.

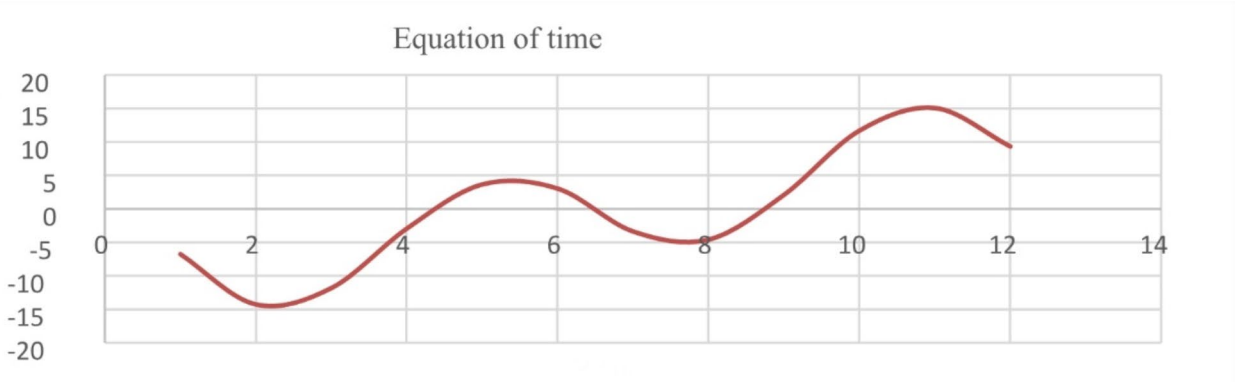

Fig. 5. Equation of Time.

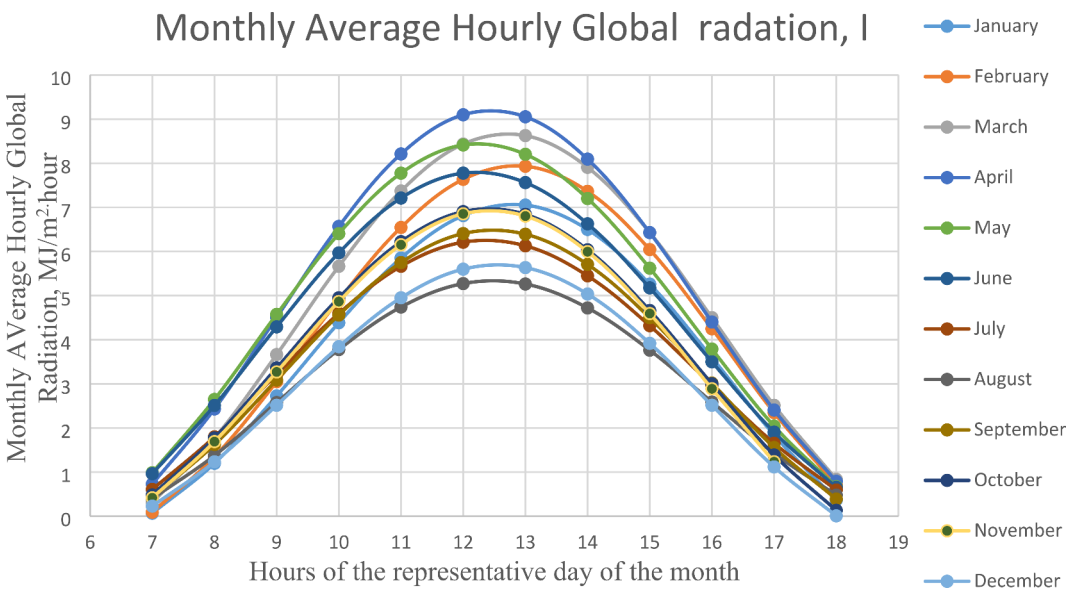

Fig. 6. Monthly Variation of Horizontal Surface Global Solar Radiation.

Minimum and maximum hourly global radiation at location 37^0 E and 11.6^0 N Baihr Dar city was recorded in August, 5.27 MJ/m^2.hour and April, 9.09 MJ/m^2.hour respectively.

Figure 7 shows that the average hourly diffuse radiation for each representative day of months in a year. Minimum and maximum hourly diffuse radiation at location 37^0 E and 11.6^0 N Baihr Dar city was recorded in January, 1.105MJ/m^2.hr and June,2.302 MJ/m^2.hr respectively. Figure 8 shows horizontal surface beam radiation (Monthly Average hourly).

The maximum monthly average hourly global radiation and corresponding diffused monthly average hourly radiation for a particular month April are given in Fig. 9. Likewise, the maximum monthly average hourly-diffused radiation and corresponding monthly average hourly-diffused radiation for a particular month April are given in Fig. 10.

3.2. Average solar radiation on a sloped surface

As per Liu and Jordan's investigation, the radiation available on the tilted surface involves beam, diffuse, and reflected radiation from the ground[1].

The total solar radiation (I_T) on a surface tilted at slope β from the horizontal[4]:

$$I_T = I_b R_b + I_d \left(\frac{1+cos\beta}{2}\right) + I\,(\rho\,)\left(\frac{1-cos\beta}{2}\right) \tag{13}$$

Mathematically,

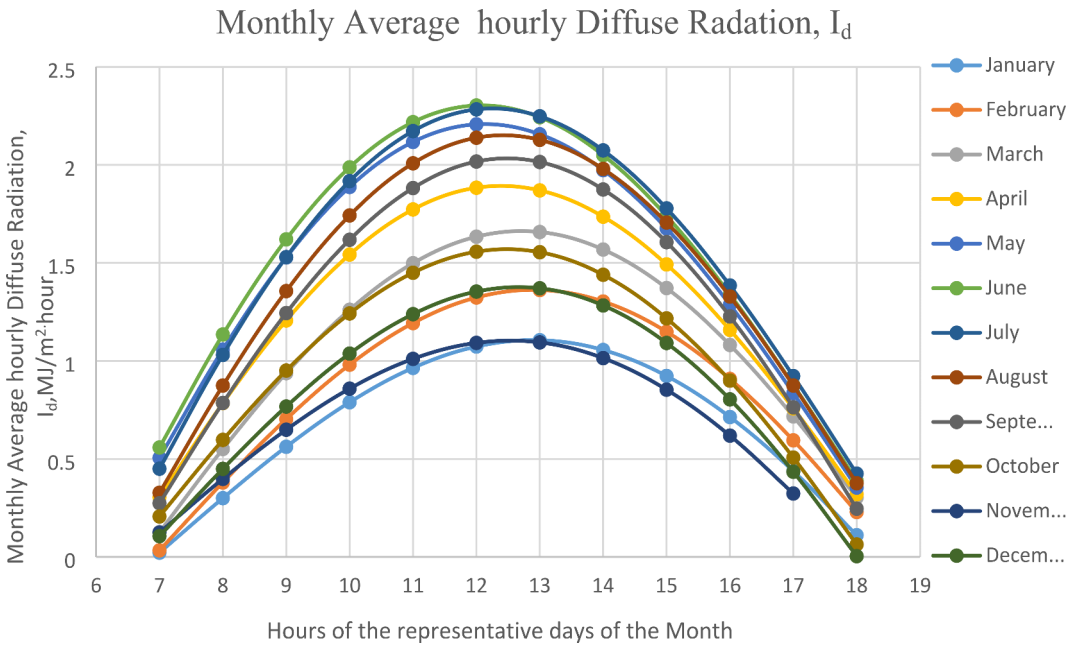

Fig. 7. Monthly Variation of Horizontal Surface Diffuse Solar Radiation.

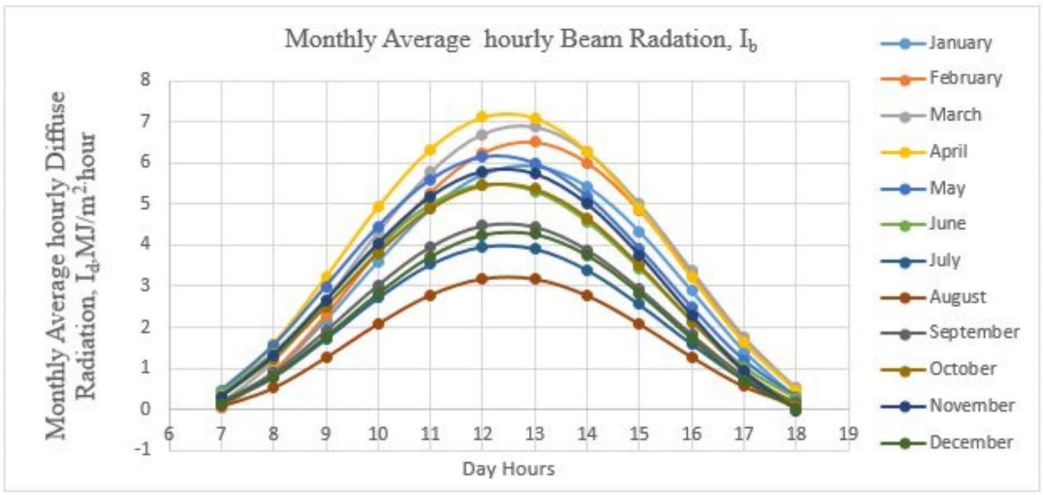

Fig. 8. Monthly Variation of Horizontal Surface Beam Solar Radiation.

$$R = \frac{\text{Tilted surfaced total radiation}}{Horizontal\ surface\ total\ radiation}$$

$$R = \frac{I_b}{I}R_b + \frac{I_d}{I}\left(\frac{1+cos\beta}{2}\right) + \rho\left(\frac{1-cos\beta}{2}\right) \tag{14}$$

Beam radiation factor (Rb) is quantified by the average daily beam on the tilted surface over that on a.

Horizontal surface for the month. For northern hemisphere surfaces sloped toward the equator, with $y = 0^0$ the equations become[24,25]

$$R_b = \frac{\cos(\varnothing - \beta)\,cos\delta\ sin\omega' s + (\pi/180)\omega' s\sin(\varnothing - \beta)\sin\delta}{cos\varnothing\ cos\delta\sin\omega s + \left(\frac{\pi}{180}\right)\omega\, s\, sin\varnothing\sin\delta} \tag{15}$$

Where,

$$\omega' s = \min\left[\cos^{-1}(-\tan\varnothing\tan\delta)\ or\ \cos^{-1}(-\tan(\varnothing - \beta)\tan\delta\right) \tag{16}$$

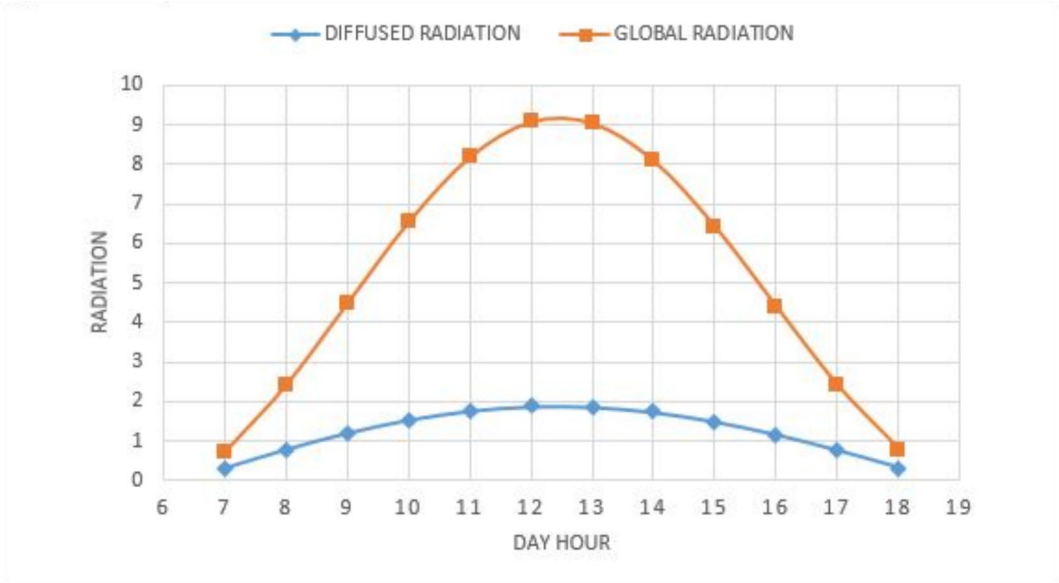

Fig. 9. Radiation (MJ/m2) for April, 2022 on Horizontal Surface Vs Day Hour.

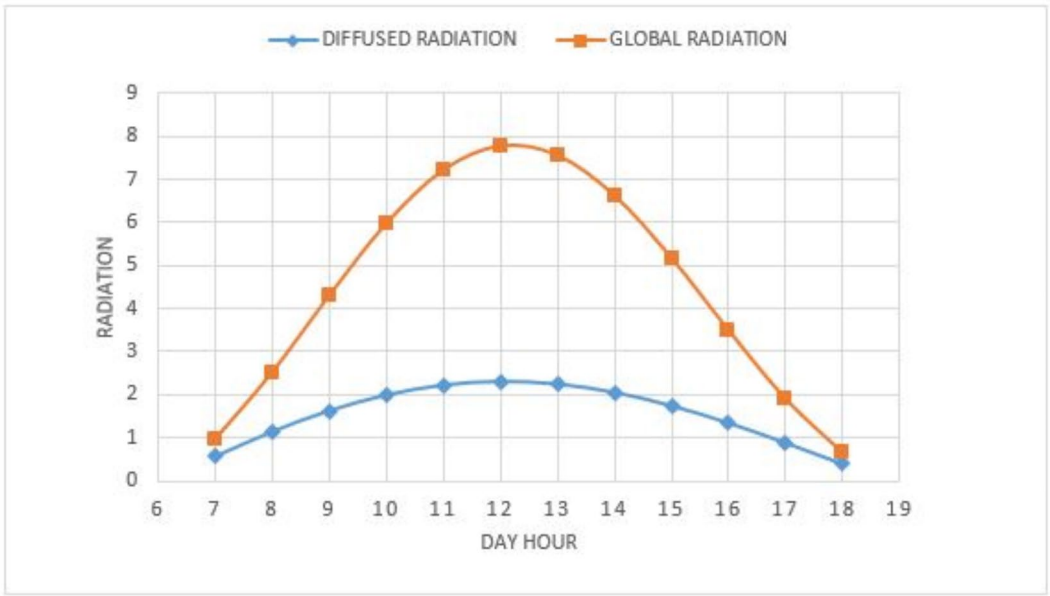

Fig. 10. Radiation (MJ/m2) for June 2022 on Horizontal Surface vs. day Hour.

Optimum tilt angle

$$(\beta_{opt} = \varnothing + (10 - 15)^{\circ}) \tag{17}$$

$$\beta_{opt} = 11.6 + 15 \cong 26.6^{\circ}$$

Diffuse radiation factor (Rd).

$$R_d = \frac{1 + cos\beta}{2} \tag{18}$$

Reflected radiation factor (Rr)

Months	Sunset hour angle one
January	85.5
February	87.3
March	89.5
April	91.9
May	94.0
June	95.0
July	94.6
August	92.8
September	90.5
October	88.0
November	85.9
December	85.0

Table 6. Sunset hour angle one.

Months	Sunset hour angle two
January	95.87801
February	93.5338
March	90.64823
April	87.4535
May	84.76878
June	83.44181
July	84.03949
August	86.32447
September	89.40568
October	92.59738
November	95.26728
December	96.54662

Table 7. Sunset hour angle two.

$$R_r = \frac{1 - cos\beta}{2} \tag{19}$$

Similarly, for daily radiation reach on the tilt surface

$$H_T = H_b R_b + H_d R_d + H\left(\rho\right) R_r$$

$$\rho = 0.7 \text{ for January and February, } 0.4 \text{ for December and March and}$$

$$0.2 \text{ for other months using isotropic assumption [21]}$$

Tables 6 and 7 present $\omega's$ one and $\omega's$ two respectively and Table 8 lists the minimum value.

3.3. Solar radiation on sloped surface data description

The available beam, diffuse, and total solar radiation for tilted surface toward the equator in the northern hemisphere, azimuth angle $\gamma = 0^\circ$. As per this investigation, the following summary description shows detailed available radiation values.

The solar radiation for each representative day of a year month (beam, diffuse, and total) reached on the tilted surface are listed in Table 9 and compared in Fig. 11. As per the analysis, the maximum possible total solar radiation reach on the tilt surface is 48.3 MJ/m^2. day (January) while the maximum global solar radiation reaches the horizontal surface 42.56 MJ/m^2.day (April).

Figure 12 shows the average hourly total radiation for each representative day of months in a year. The highest hourly total radiation at location 37^0 E and 11.6^0 N Baihr Dar city reach on the tilt surface is recorded in February, 9.14 MJ/m^2.hour at 1:00 pm.

Furthermore, Figs. 13 and 14 depicts the highest hourly beam and diffuse radiation reached in January, 7.4 MJ/m^2.hour at 0:00 pm (noon), and in June, 2.178 MJ/m^2.hour at 0:00 pm (noon) respectively. In addition, Table 10 compares different assessment results selected from the literature.

Months	Minimum Sunset hour angle
January	85.5
February	87.3
March	89.5
April	87.4
May	84.8
June	83.4
July	84.0
August	86.3
September	89.4
October	88.0
November	85.9
December	85.0

Table 8. Min Sunset hour angle.

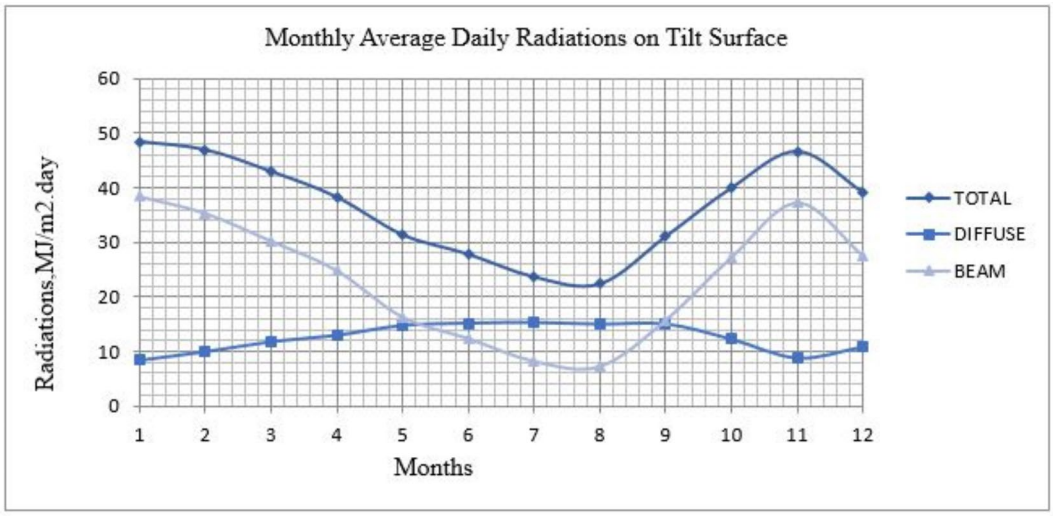

Fig. 11. Monthly Variation of Tilt Surface Beam, Diffuse, and Global Solar Radiation.

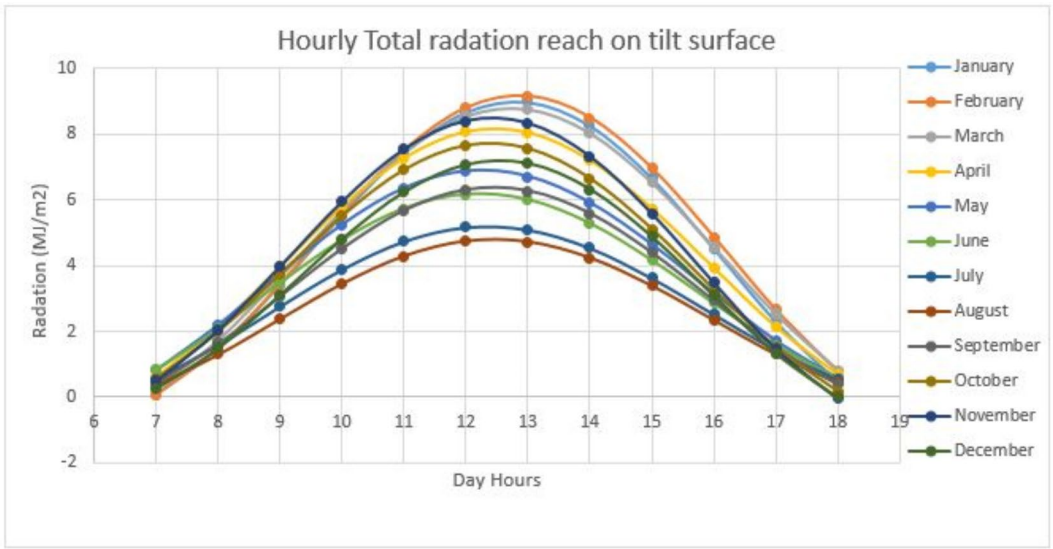

Fig. 12. Hourly Variation of Tilt Surface Total Solar Radiation.

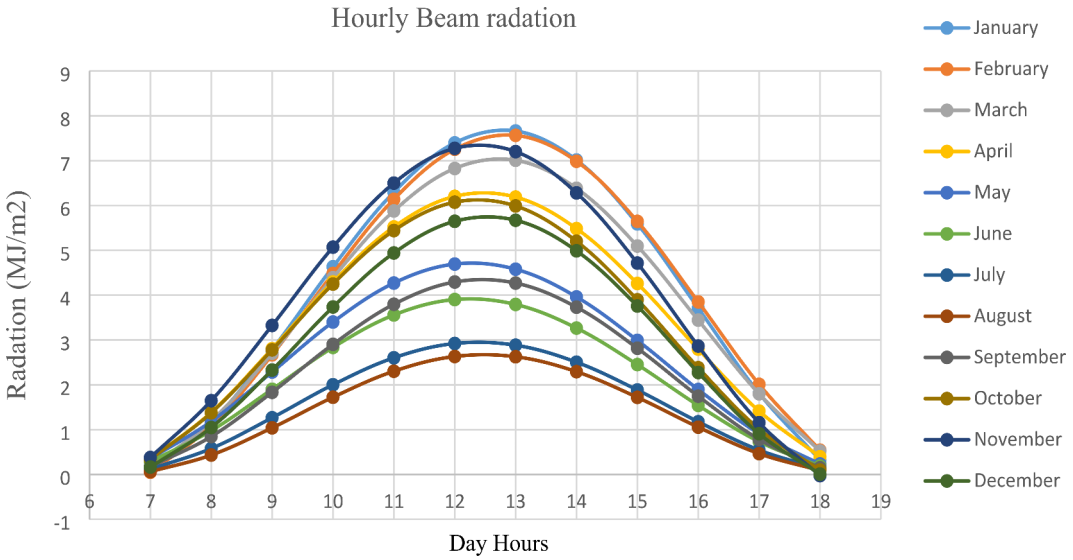

Fig. 13. Hourly Variation of Tilt Surface Beam Solar Radiation.

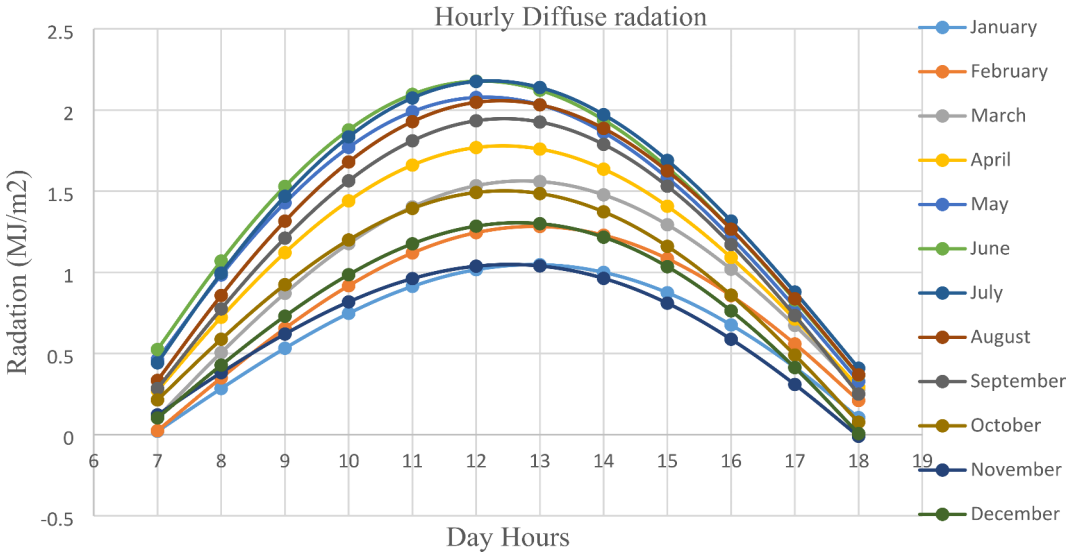

Fig. 14. Hourly Variation of Tilt Surface Diffuse Solar Radiation.

4. Conclusion

This dataset offers insightful information about Ethiopia's Bahir Dar City's solar energy potential. For five years, beam, diffuse, and global solar radiation were analyzed on both horizontal and inclined surfaces. This data is vital for supporting solar energy applications and research in the area. With plenty of sunshine and ground-level solar radiation, Bahir Dar has a tremendous potential for solar energy, as evidenced by the data. Climate modeling, agricultural planning, and the optimization of solar panel positions and efficiency for renewable energy generation can all benefit from this information. Scholars can utilize this information for additional analysis and development to enhance their own research on solar energy. These insights can also be used by industry experts and policymakers to establish strategies, shape actions pertaining to sustainable energy solutions, and influence evidence-based decision-making. All things considered, this extensive dataset advances our knowledge of Bahir Dar's solar energy characteristics and availability. It is a useful tool that supports Ethiopia's and other countries' increasing interest in and move toward renewable energy sources.

The assessment of solar energy potential in Bahir Dar City, Ethiopia, conducted by analyzing solar radiation data from 2018 to 2022, the study has uncovered the significant untapped solar resources available in the city. The researchers' analysis revealed that Bahir Dar experiences the highest global solar radiation on the horizontal surface in March, with an average daily value of approximately 42.56 MJ/m2. Interestingly, June had the lowest diffuse radiation, measured at 16.2 MJ/m2.day, indicating the prevalence of clear skies during this period.

Months	Beam on tilt surface(MJ/m2/day)	Diffuse radiation on tilt surface(MJ/m2/day)	Total radiation on tilt surface (MJ/m2/day)
January	38.4	8.5	48.3
February	35.3	10.0	46.9
March	30.2	11.8	42.9
April	24.8	13.0	38.3
May	16.3	14.7	31.4
June	12.	15.2	27.9
July	8.2	15.3	23.7
August	7.2	15.0	22.5
September	15.7	15.0	31.1
October	27.3	12.3	39.9
November	37.2	8.9	46.5
December	27.4	10.9	39.0

Table 9. Tilt surface (Monthly Average Daily) Total, Beam, and diffuse radiation MJ/m2.day.

Author (s)	Study area	Maximum Result (KWH/m2).
Muhammad Zahid Samsudin et al. [33]	Johor, Malaysia	7.15
Q. Hassan et al.[34]	Erbil, Iraq	7.34
	Anbar, Iraq	8.34
	Basra, Iraq	7.5
	Baghdad, Iraq	7.8
C. Venkatachalam et al. [25]	Adama, Ethiopia	6.64
This study	Bahir Dar, Ethiopia	11.8

Table 10. Global radiation (Monthly Average daily) selected from the literature.

These findings hold important implications for the strategic design and optimization of solar energy systems, as developers can leverage the seasonal and diurnal variations in solar radiation to maximize energy generation.

The study's predictions of the beam, diffuse, and total radiation on tilted collector surfaces further enhance the understanding of Bahir Dar's solar energy potential. The analysis showed that the highest possible total radiation (monthly average daily) on a tilted surface towards the equator in the northern hemisphere is 48.3 MJ/m2.day in January, while the highest possible total radiation (monthly average hourly) is 9.14 MJ/m2.hour in February at 1:00 pm. These remarkable findings underscore the significant potential for the widespread adoption of solar energy technologies in Bahir Dar, empowering the region to embrace a more sustainable and resilient energy future. As the global energy landscape continues to evolve, Bahir Dar's solar energy potential stands as a shining example of the transformative power of renewable energy solutions.

Data availability

The data that supports the findings of this study are available within the article.

Received: 24 February 2024; Accepted: 26 September 2024
Published online: 01 October 2024

References

1. Marzband, M., Javadi, M., Pourmousavi, S. A. & Lightbody, G. An advanced retail electricity market for active distribution systems and home microgrid interoperability based on game theory, Electr. *Power Syst. Res.* **157**, 187–199 (2018).
2. Administration, U. E. I. *Int. Energy Outlook*, 2017 overview, [Online] Available: www.eia.gov/.
3. Ramachandra, T., Jain, R. & Krishnadas, G. Hotspots of solar potential in India. *Renew. Sustain. Energy Rev.* **15**(6), 3178–3186 (2011).
4. Ahmadi, M. et al. Solar power technology for electricity generation: a critical review. *Energy Sci. Eng.* **6**, 340e361 (2018).
5. Yushchenko, A., de Bono, A., Chatenoux, B., Kumar Patel, M. & Ray, N. Gis-based assessment of photovoltaic (pv) and concentrated solar power (csp) generation potential in west africa. *Renew. Sustain. Energy Rev.* **81**, 2088–2103 (2018).
6. Blanc, P., Espinar, B., Geuder, N., Gueymard, C. & Meyer, R. Direct normal irradiance related definitions and applications: the circumsolar issue. *Sol Energy*. **110**, 561e577 (2014).
7. Marzband, M., Fouladfar, M. H., Akorede, M. F., Lightbody, G. & Pouresmaeil, E. Framework for smart transactive energy in home-microgrids considering coalition formation and demand side management, Susta. *Cities Soc.* **40**, 136e154 (2018).
8. El Mghouchi, Y., El Bouardi, A., Choulli, Z. & Ajzoul, T. Estimate of the direct, diffuse and global solar radiations. *Int. J. Sci. Res. (IJSR)*. **33**, 1449–1457 (2014).
9. Asilevi, P. J., Quansah, E., Amekudzi, L. K., Annor, T. & Klutse, N. A. B., Modeling the spatial distribution of Global Solar Radiation (GSR) over Ghana using the ˚Angström-Prescott sunshine duration model, Scientific African 4 1–12 (2019)e0 0 094. (2019).
10. Quansah, E. et al. Empirical models for estimating global solar radiation over the Ashanti region of Ghana. *J. Solar Energy*. **2014**(3), 1–6. https://doi.org/10.1155/2014/897970 (2014).

11. Iqbal, M. in: An Introduction to Solar Radiation, Elsevier, p. 408, doi: 10.1016/B978-0-12- 373750- 2.X5001- 0. ISBN 9780123737502, https://doi.org/. (1983).
12. Andrea, Y., Pogrebnaya, T. & Kichonge, B. Effect of Industrial Dust Deposition on Photovoltaic Module performance: experimental measurements in the Tropical Region. *Int. J. Photoenergy*. **1892148**, 10. pageshttps://doi.org/ (2019).
13. Paudyal, B. R. & Shakya, S. R. Dust accumulation effects on efficiency of solar PV modules for offgrid purpose: a case study of Kathmandu. *Sol Energy*. **135**, 103–110. https://doi.org/ (2016).
14. Yusuf, A. Characterization of Sky conditions using clearness index and relative Sunshine Duration for Iseyin, Nigeria. *Int. J. Phys. Sci. Res.* **1**(1), 53–60 (2017).
15. Babatunde, E. B. & Aro, T. O. Relationship between clearness indexand cloudiness indexat a tropical station (Ilorin, Nigeria). *Renew. Energy*. **6**(7), 801–805 (1995).
16. Olabi, A. G. & Abdelkareem, M. A. Renewable energy and climate change. *Renew. Sustain. Energy Rev.* **158**, 112111 (2022).
17. Castillo, C. P., e Silva, F. B. & Lavalle, C. An assessment of the regional potential for solar power generation in EU-28. *Energy Pol.* **88**, 86–99 (2016).
18. Tegenu Argaw woldegiyorgis. Natei Ermias Benti, Mesfin Diro Chaka, Addisu Gezahegn Semie, Birhanu Asmerom Habtemicheal, Abera Debebe Assamnew, Ashenafi Admasu Jembrie, Harnessing solar power: Predicting photovoltaic potential in fiche, oromia, Ethiopia with artificial neural networks. *Sci. Afr.* **21**, e01884 (2023).
19. Duffie, J. A. & Beckman, W. A. Solar Engineering of Thermal Processes, Wiley Inter. science, New York. fourth edition. (1991).
20. Iqbal, M. An Introduction to Solar Radiation, academic press, The University of British Columbia Vancouver, British Columbia, Canada, First Edition. (1983).
21. John, A., Duffie, W. A. & Beckman Solar Energy Laboratory: 4th ed., (2013).
22. G.N. Tiwari Arvind Tiwari Shyam, Energy Systems in Electrical Engineering, (2016).
23. Akpabio & Etuk *Relation-ship between Global Solar Radiation and Sunshine Duration for Onne* (Nigeria, 2003).
24. Soulayman & Sabbagh Optimum tilt angle at tropical region. *Int. J. Renew. Energy Dev.* **4** (2015).
25. Venkatachalam, C. et al. Dataset of solar energy potential assessment for Adama city (Ethiopia). (2019).
26. Sabbagh Syigh and El- Salam, Estimation of the total solar radiation from meteorological data, (1977).
27. Bahir Dar Metrology Agency.
28. Chie, J., Rahman, M. & Adli, R. January, Renewable energy: a brief review renewable energy: a brief review, **030028**, no. (2023).
29. Area, N., Region, O. & Woldegiyorgis, T. A. Analysis of solar PV energy systems for rural villages of, **6**, 1, pp. 13–22, (2019).
30. Jain, A., Das, P., Yamujala, S., Bhakar, R. & Mathur, J. Resource potential and variability assessment of solar and wind energy in India. *Energy*. **211**, 118993 (2020).
31. OLANREWAJU OLUKEMI SONEYE-AROGUNDADE1. And BERNHARD RAPPENGLU¨ CK estimation of diffuse Solar Radiation models for a Tropical Site in Nigeria. *Pure Appl. Geophys.* **180**, 3385–3400 (2023).
32. Basharat Jamil, N. & Akhtar October, Comparative analysis of diffuse solar radiation models based on sky-clearness index and sunshine period for humid-subtropical climatic region of India: a case study, renewable and sustainable energy reviews. **78**, Pages 329–355 (2017).
33. Muhammad Zahid Samsudin. Assessment of Solar Energy Potential in Johor, Malaysia. *J. Des. Sustainable Environ.* **3 No**(1), 1–6 (2021).
34. Hassan, Q. et al. Assessment the potential solar energy with the models for optimum tilt angles of maximum solar irradiance for Iraq. *Case Stud. Chem. Environ. Eng.* **4**, 100140 (2021).

Acknowledgements

This work supported by Bahirdar metrology agency, Bahirdar, Ethiopia for helping to gather the available sunshine hour radiation value.

Author contributions

A.G, T.G, A.B: Significant contribution to the concept, analysis and interpretation of the data and writing of the article.R.B, T.S , H.M: Critically drafted and revised the article for significant intellectual content and made a significant contribution to the concept of the article.

Funding

This research did not receive any specific grant from funding agencies in the public, commercial, or not-for-profit sectors.

Declarations

Competing interests

The authors declare no competing interests.

Additional information

Correspondence and requests for materials should be addressed to R.B.N.